

# THE INFLUENCE OF HIGH MULTIPLICITIES AT RHIC <sup>1</sup> ON THE GAMOV FACTOR

*D.V. Anchishkin* <sup>a,b,2</sup>, *W.A. Zajc* <sup>c,3</sup>, *G.M. Zinovjev* <sup>b,4</sup>

<sup>a</sup>CERN TH-Division, CH-1211 Geneva 23, Switzerland

<sup>b</sup>Bogolyubov Institute for Theoretical Physics,  
National Academy of Sciences of Ukraine  
252143 Kiev-143, Ukraine

<sup>c</sup>Nevis Laboratories, Columbia University,  
Irvington, NY 10533, USA

## Abstract

The corrections for two-pion correlations due to electromagnetic final-state interactions at high secondary multiplicities are investigated. The analysis is performed by solving the Schrödinger equation with a potential which is dictated by the multi-particle environment. Two different post-freeze-out scenarios are examined. First, for a uniformly spread environment of secondary particles, a screened Coulomb potential is exploited. It is shown that the presence of a static and uniform post-freeze-out medium results in a noticeable deviation from the standard Gamov factor. However, after going to a more realistic model of an expanding pion system, this conclusion changes drastically. We argue that the density of the secondary pions  $n_\pi(t, R)$ , where  $R$  is a distance from the fireball, is bounded from above by  $n_\pi(t, R) \leq \text{const}/R^2$  for all times  $t$ . Then, a two-particle scalar potential which is found as a solution of the Maxwell equation for non-uniform medium replaces the screened one. Even this upper limit does not result in an essential deviation from the Gamov correction.

---

<sup>1</sup> RHIC is an abbreviation of “relativistic heavy-ion collisions”.

<sup>2</sup> E-mail: Dmitry.Anchishkin@cern.ch or/and Dmitry.Anchishkin@ap3.bitp.kiev.ua

<sup>3</sup> E-mail: ZAJC@nevis1.nevis.columbia.edu

<sup>4</sup> E-mail: GEZIN@ap3.bitp.kiev.ua

# 1 Introduction

Two-particle correlations provide information about the space-time structure and dynamics of the emitting source [1]. Considering the correlations that occur in relativistic heavy-ion collisions one usually assumes that: (i) the particles are emitted independently (or the source is completely chaotic), and (ii) finite multiplicity corrections can be neglected. Then the correlations reflect a) the effects from symmetrization (antisymmetrization) of the wave function and b) the effects that are generated by the final-state interactions of the detected particles between themselves and with the source. At first sight one can regard the final-state interactions (FSI) as a contamination of the ‘pure’ particle correlations. It should be pointed out, however, that the FSI depend on the structure of the emitting source and thus provide information about the source dynamics as well. In fact, this was proved by intensive investigations during the last twenty years of two-particle and source-particle FSI [1, 2] (for recent publications see, for example, on two-particle FSI, [3, 4] and references therein; on source-particle FSI, [5, 6] and references therein).

Actually, the former approaches accounting for FSI deal with the secondaries in empty post-freeze-out space. Meanwhile, in recent SPS experiments, for instance Pb + Pb at  $160 \text{ GeV} \times A$ , some 800–900 secondary charged pions are created which form obviously a plasma-like post freeze-out medium. Therefore, one might expect that the FSI of two separate pions, at this collision energy, and of course at the energies of the forthcoming RHIC and LHC colliders, would be strongly influenced by the environment formed by other particles. The goal of the present paper is to estimate how large are the consequences on the Coulomb final-state interactions due to the presence of a large number of secondary charged particles. To be as independent as possible from source models, we chose the estimation of the Gamov factor as a standard quantity, which serves as a measure of the Coulomb FSI.

The fundamental observable for intensity interferometry in hadron physics is the relative momentum spectrum of identical particles. For two like-sign pions, the modifications to the spectrum by the final-state Coulomb interaction result in a correction that has typically been considered as tractable with high accuracy. This assumption was based on the significantly different length scales between strong ( $\propto 1/m_\pi$ ) and Coulomb ( $\propto 1/m_\pi\alpha$ ) interactions [7, 8] (here  $m_\pi$  is the pion mass and  $\alpha$  represents the fine structure constant). The correction may then be treated on the basis of the Schrödinger equation, resulting in the well-known Gamov factor  $G(\mathbf{q})$

$$G(|\mathbf{q}|) = |\psi_{\mathbf{q}}(\mathbf{r} = 0)|^2 = \frac{2\pi\eta}{e^{2\pi\eta} - 1} , \quad (1)$$

where  $\psi_{\mathbf{q}}(\mathbf{r})$  is the two-particle wave function,  $\eta = \alpha m_\pi / |\mathbf{q}|$ , and  $\mathbf{q}$  is the relative momentum of the particles.

The nominal quantity expressing the correlation function in terms of experimental distributions [1] is

$$C(\mathbf{k}_1, \mathbf{k}_2) = \frac{P_2(\mathbf{k}_1, \mathbf{k}_2)}{P_1(\mathbf{k}_1) P_1(\mathbf{k}_2)} , \quad (2)$$

where  $P_1(\mathbf{k}) = E d^3N/d^3k$  and  $P_2(\mathbf{k}_1, \mathbf{k}_2) = E_1 E_2 d^6N/(d^3k_1 d^3k_2)$  are single- and two-particle cross-sections. For point-like emitters it can be expressed (due to the factorization of the corresponding matrix element) in terms of a product of the Gamov factor to the model

correlations [2, 3]:

$$C(\mathbf{k}_1, \mathbf{k}_2) = G(|\mathbf{k}_1 - \mathbf{k}_2|) C_{\text{model}}(\mathbf{k}_1, \mathbf{k}_2) . \quad (3)$$

It should be mentioned that, in the centre of mass of the pair the relative pion momentum  $|\mathbf{q}| = 2|\mathbf{k}|$ , with  $\mathbf{k} = \mathbf{k}_1 = -\mathbf{k}_2$ , coincides with invariant relative momentum  $q_{\text{inv}} \equiv [(k_1 + k_2)^2 - 4m_\pi^2]^{1/2}$ , where  $k_1$  and  $k_2$  are the pion four-momenta in an arbitrary frame.

We consider corrections due to the Coulomb final-state interactions in a common scheme in which we do not take into account the finite-size of the fireball (for a consistent treatment of the source finite-size effects, see for example [3]). This means that we calculate the correction factor in accordance with the formula  $G_{\text{corr}}(|\mathbf{q}|) = |\psi_{\mathbf{q}}(\mathbf{r} = 0)|^2$ , where now  $\psi_{\mathbf{q}}(\mathbf{r})$  is obtained from a numerical solution of the Schrödinger equation with the two-particle Coulomb potential *distorted by a multipion environment*. Since, as shown in [3], the finite size of the emission source softens the manifestation of the FSI, the ‘Gamov factor’ tends to overestimate the FSI effects and therefore it is the most sensitive quantity for deviations from the standard two-particle Coulomb interaction.

## 2 Static multiparticle environment

In the high multiplicity case, when a post-freeze-out multipion environment cannot be neglected, the relation between the two-particle electromagnetic potential  $\phi(\mathbf{r})$  and the local charge density is given by

$$\nabla^2 \phi(\mathbf{r}) = -4\pi e(n^{(+)} - n^{(-)}) , \quad (4)$$

where  $e = \sqrt{\alpha}$  is the elementary charge; the density of charged pions  $n^{(\pm)}$  is related to that of neutral pions  $n^{(0)}$  via a Boltzmann factor:

$$n^{(\pm)} = n^{(0)} \exp\left(\mp \frac{e\phi}{T_f}\right) , \quad (5)$$

The density  $n^{(0)}$  of  $\pi^0$ -mesons at the freeze-out temperature  $T_f$  coincides with the equilibrium density of charged pions in the absence of Coulomb interactions (we consider symmetrical nuclear matter). In the limit  $e\phi \ll T_f$ , Eq.(5) can be rewritten as

$$n^{(\pm)} = n^{(0)} \left(1 \mp \frac{e\phi}{T_f}\right) \quad (6)$$

(this requires that the pions are not closer than  $\sim 10^{-2}$  fm to one another at  $T_f \approx 200$  MeV), so that

$$\nabla^2 \phi(\mathbf{r}) = \frac{4\pi e^2}{T_f} (2n^{(0)}) \phi(\mathbf{r}) . \quad (7)$$

The solution of this equation is well known and given by a screened Coulomb potential

$$\phi_{\pi^\pm}(r) = \pm e \frac{e^{-r/R_{\text{scr}}}}{r} , \quad (8)$$

where

$$\frac{1}{R_{\text{scr}}} = \sqrt{\frac{8\pi}{3}} \alpha \cdot \sqrt{\frac{n_\pi}{T_f}} \quad (9)$$

with the total pion density  $n_\pi = 3n^{(0)}$ . Thus, for like-sign pions the potential energy reads

$$U_{\pi\pi}(r) = \frac{\alpha}{r} \exp\left(-\frac{r}{R_{\text{scr}}}\right). \quad (10)$$

To evaluate the correction factor we use the screened Coulomb potential (10) to solve the Schrödinger equation numerically, for the two choices: 1)  $n_\pi = 0.25 \text{ fm}^{-3}$  and 2)  $n_\pi = 0.03 \text{ fm}^{-3}$ . (From now on we shall quote these two cases as “*LHC*” and “*SPS*” freeze-out conditions, respectively.) Taking  $T_f = 190 \text{ MeV}$ , for example, we obtain from Eq. (9) screening radii  $R_{\text{scr}} \approx 7.9 \text{ fm}$  (*LHC*),  $R_{\text{scr}} \approx 22.4 \text{ fm}$  (*SPS*), respectively. For completeness of illustration we also consider the intermediate case  $R_{\text{scr}} \approx 19.3 \text{ fm}$ .

The results of these calculations are plotted in Fig. 1 together with the standard Gamov factor. We see that a substantial correction to the standard Gamov factor would be required even for the existing experimental data if one adopts the idealized picture of a uniform post-freeze-out density of the environment.

It is interesting to point out that the correction factor  $G_{\text{cor}}(q)$ , which was evaluated for the same screened potential using the quasi-classical approximation [9], does not make a big difference with the correction factor in Fig. 1.

Actually, what we really learned from the consideration of this idealized scenario is that a cancellation of the Coulomb potential tail (by screening) results in an increase of the correction factor in the region of small relative momentum ( $q \leq 50 \text{ MeV}$ ), as can be seen from Fig. 1. Thus the long-distance behaviour of the potential is responsible for the dramatic deviation of the correction factor from the standard Gamov factor at small relative momenta. On the other hand, the tail of the two-particle potential gives the main contribution to interactions when the particles are at large distances from one another, where in turn the density of secondary particles is small in the realistic picture. To keep this qualitative speculation as a thread we next turn to a more realistic calculation, explicitly incorporating expansion.

### 3 Expansion scenario

In the previous scenario the whole position space was filled by particles with a constant density; this is certainly an unrealistic approximation (idealization). In order to take into account post-freeze-out expansion of the pion system, we parametrise the pion density as

$$n(R) = n_f \frac{R_f^2}{R^2}, \quad (11)$$

where  $n_f$  is the freeze-out pion density and  $R_f$  is the freeze-out radius. Indeed, the spatial volume of the expanding pion system in the solid angle  $\Omega$  increases as  $\Delta V = \Omega \cdot R^2 \cdot \Delta R$ , where  $R$  is the distance from the centre of the fireball and  $\Delta R$  is the thickness of the layer, which we keep constant. Then, if the number of particles  $\Delta N$  in this volume is constant, the density reads:  $n(R) = \Delta N / (\Omega \cdot R^2 \cdot \Delta R) = \text{const} / R^2$ . Thus, the model (11) implies that all particles have the same modulus of radial velocity. As we shall see further, such a model still means an overestimation of the particle density.

To support our assumption (11) let us consider a classical pion phase-space distribution. After freeze-out it satisfies the collisionless Boltzmann kinetic equation

$$\frac{\partial f(x, p)}{\partial x_0} + \mathbf{v} \cdot \nabla f(x, p) = 0, \quad (12)$$

where  $\mathbf{v} = \mathbf{p}/p_0$  is the velocity of the particle and  $p_0 = \omega(\mathbf{p}) \equiv \sqrt{m_\pi^2 + \mathbf{p}^2}$ . We look for the expansion solution of this equation, which can be fixed by asymptotic condition, for instance  $\lim_{t \rightarrow \infty} f(t, \mathbf{x} = 0; \mathbf{p}) = 0$ . A solution of this type can be written in the form

$$f(t, \mathbf{R}, \mathbf{p}) = f_0(\mathbf{R} - \mathbf{v}t, \mathbf{p}), \quad (13)$$

where  $f_0(\mathbf{R}, \mathbf{p})$  is the initial distribution ( $t = 0$ ). For the sake of simplicity, we take an isotropic initial distribution in position and momentum spaces: just before freeze-out the particles were distributed (a) in accordance with Boltzmann's law in momentum space, and (b) in accordance with a Gaussian distribution in position space. The classical kinetic equation is quite sufficient to describe the *collective* (!) behaviour of the pion system after freeze-out. Hence, we assume that the system, at time  $t = 0$ , occupies the phase space according to the distribution function

$$f_0(\mathbf{R}, \mathbf{p}) = n_0(\mathbf{R})g_0(\mathbf{p}), \quad (14)$$

where

$$n_0(\mathbf{R}) = \frac{N_\pi}{(2\pi R_f^2)^{3/2}} \exp\left(-\frac{R^2}{2R_f^2}\right) \quad (15)$$

with  $\int d^3R n_0(\mathbf{R}) = N_\pi$ , and

$$g_0(\mathbf{p}) = \frac{2\pi^2}{m_\pi^2 T_f K_2\left(\frac{m}{T_f}\right)} \exp\left(-\frac{\sqrt{m_\pi^2 + \mathbf{p}^2}}{T_f}\right) \quad (16)$$

with  $\int [d^3p/(2\pi)^3] g_0(\mathbf{p}) = 1$ . Here  $N_\pi$  is the total number of pions,  $T_f$  and  $R_f$  are the temperature and the mean radius of the system at time  $t = 0$  (freeze-out), respectively,  $m_\pi$  is the pion mass and  $K_2$  is a Bessel function of imaginary argument.

The spatial distribution of the particles at time  $t$  is determined by integrating the distribution function (13) over the momentum variable

$$n(t, \mathbf{R}) = \int \frac{d^3p}{(2\pi)^3} n_0\left(\mathbf{R} - \frac{\mathbf{p}}{\omega(\mathbf{p})}t\right) g_0(\mathbf{p}). \quad (17)$$

Because of the spherical symmetry, it is reasonable to look at the radial density of pions

$$n_{\text{sph}}(t, R) \equiv 4\pi R^2 n(t, R). \quad (18)$$

This quantity may be treated as the number of pions in the shell with unit thickness at time  $t$  and at a distance  $R = |\mathbf{R}|$  from the fireball centre. Hence,  $n_{\text{sph}}(t, R)$  is a one-dimensional spatial distribution function and, evidently, the area under this curve at any time is equal

to the particle number  $N_\pi$ , because of its normalization  $\int_0^\infty dR n_{\text{sph}}(t, R) = N_\pi$ . We evaluate this function in accordance with Eq. (17) for *SPS* freeze-out conditions:  $n_f = 0.03 \text{ fm}^{-1/3}$ ,  $T_f = 190 \text{ MeV}$  and  $R_f = 7.1 \text{ fm}$ . The results of this calculation at different times  $t$  are given in Fig. 2. It shows that the spherical distribution is always almost Gaussian-like and the velocity of the distribution maximum is very close to the velocity of light. The horizontal line (see Fig. 2) denotes a constant spherical density  $4\pi R^2 n(R) = \text{const}$ . This line is nothing more than the 3-dimensional spatial density  $n(R) = \text{const}'/R^2$  (for the *SPS* freeze-out conditions  $\text{const}' \approx 85/4\pi$ ). It follows that, at any time  $t$ , for the post-freeze-out particle density  $n(t, R)$  the upper limit is valid

$$n(t, R) \leq n_f \frac{R_f^2}{R^2}, \quad (19)$$

where  $n_f = \max\{n(t=0, R)\}$  and the equality is reached for an expanding system where the radial particle velocities are equal. Because of momentum dispersion in the post-freeze-out pion system, the pion density (11) is an *essential overestimation* of the real density, which is formed by the comoving multipion environment. Hence, adopting the stationary density dependence (11) we overestimate the influence of the environment, and consequently overestimate a distortion of the Coulomb FSI in the expansion scenario. On the other hand, this approach provides us with a possibility to consider a stationary post-freeze-out environment even in the frame of the non-stationary expansion scenario (see Fig. 2).

Adopting the parametrization (11), we get Eq. (7), where the pion density  $n_\pi$  now depends on  $R$ :

$$\nabla^2 \phi(\mathbf{r}) = \frac{8\pi\alpha}{3T_f} n(R) \phi(\mathbf{r}), \quad (20)$$

where we put  $n^{(0)} \approx n_\pi/3$  as before ( $n_f = n_\pi$ ). Inserting the pair centre of mass distance  $R$  together with the distance  $r$  between two detected particles, we have, in the classical approach:

$$R \approx R_f + v_{\text{cm}} \cdot t, \quad r \approx v_{\text{rel}} \cdot t, \quad (21)$$

where  $v_{\text{cm}}$  is the velocity of the two-particle centre of mass in the fireball rest frame and  $v_{\text{rel}}$  is the relative velocity of the particles ( $v_{\text{rel}} = q/m$ ,  $t = 0$  is fixed on the freeze-out hyper-surface). Eliminating the time from the approximate equalities (21) one has

$$R = R_f + \frac{v_{\text{cm}}}{v_{\text{rel}}} \cdot r, \quad (22)$$

which means that we parametrize the time evolution by the mean distance  $r$  between two detected particles.

We can thus rewrite the dependence of the pion density on  $r$  as

$$n(R(r)) = \left( \frac{v_{\text{rel}}}{v_{\text{cm}}} \right)^2 \frac{n_f R_f^2}{(r + \bar{r})^2}, \quad (23)$$

where we define the dynamical freeze-out radius

$$\bar{r} \equiv R_f \frac{v_{\text{rel}}}{v_{\text{cm}}}. \quad (24)$$

It is time to recapitulate what has been done. First, we eliminate the time dependence of the particle density, bounding it from above by a stationary non-uniform spatial distribution, in accordance with inequality (19). Then, we connect the mean distance  $R$  of the pair c.m.s. from the fireball and the mean distance  $r$  between pions, thus eliminating again the time dependence. This means that all time and  $R$  dependences are now parametrized by the variable  $r$ . If the relative velocity of the separate pions is small, then the partial time derivative  $\frac{\partial}{\partial t} = v_{\text{rel}} \frac{\partial}{\partial r}$  can be neglected. Hence, the problem is approximately reduced to a stationary one. Solving Eq. (20) with particle density from (23), one obtains the two-particle potential energy  $U(r) = e \phi(r)$ , which will then be exploited in the stationary Schrödinger equation to find a wave function. This will be the further strategy of our estimations. So, the problem of a time-dependent (expansion scenario) is reduced to a stationary one by the price of somewhat overestimating the Coulomb corrections.

Equation (20) may be rewritten as

$$\nabla^2 \phi(\mathbf{r}) = \frac{c^2(q)}{(r + \bar{r})^2} \phi(\mathbf{r}) , \quad (25)$$

where we note explicitly that when the particles are separated by large distances  $r$  the density of the multiparticle environment goes down in accordance with (23). The quantity  $c^2(q)$  is defined in the following way:

$$c^2(q) = \frac{8\pi\alpha}{3} \frac{R_f^2 n_f}{T_f} \frac{v_{\text{rel}}^2}{v_{\text{cm}}^2} . \quad (26)$$

Fixing the screening radius at freeze-out

$$R_{\text{scr}}^f = \sqrt{\frac{3T_f}{8\pi\alpha n_f}} , \quad (27)$$

we have

$$c(q) = \frac{R_f}{R_{\text{scr}}^f} \frac{v_{\text{rel}}(q)}{v_{\text{cm}}} . \quad (28)$$

In spherical coordinates, Eq. (25) can be rewritten as

$$\frac{d^2 \phi(r)}{dr^2} + \frac{2}{r} \frac{d\phi(r)}{dr} - \frac{c^2(q)}{(r + \bar{r})^2} \phi(r) = 0 . \quad (29)$$

This equation may be solved by

$$\phi(r) = \frac{e}{r} \left( \frac{\bar{r}}{r + \bar{r}} \right)^b , \quad (30)$$

where  $\phi(r)$  satisfies the boundary condition:  $\phi(r) \rightarrow e/r$  when  $r \rightarrow 0$ . The exponent  $b$  is a solution of the quadratic equation resulting from the substitution of the ansatz (30) into Eq. (29) and takes the form (assuming proper asymptotic behaviour of the potential  $\phi$ ):

$$b(q) = -\frac{1}{2} + \frac{1}{2} \sqrt{1 + 4c^2(q)} . \quad (31)$$

One has  $b \rightarrow 0$  when  $n_f \rightarrow 0$  and hence the potential  $\phi(r)$  transforms into the Coulomb potential in this case. It is shown in Figs. 3a and 3b for *LHC* and *SPS* freeze-out conditions,

respectively. In the interval of interest,  $b$  increases with increasing relative velocity, and so do deviations from a pure Coulomb field. This intriguing behaviour is directly related to the “Hubble-like” expansion implied by Eq. (22): it becomes clear if we remember that the pion density decreases (hence  $R_{\text{scr}} \rightarrow \infty$ ) with increasing distance  $R$ . The expansion thus results in modifications to the Coulomb potential that are of power-law, not exponential, form, in contrast to the static result given by Eq. (8).

The connection of the potential (30) and screened one can be found in the following way. One may treat the corrected potential obtained in Eq. (30) as an effective charge distribution

$$e_{\text{eff}} = e \left( \frac{\bar{r}}{r + \bar{r}} \right)^b, \quad (32)$$

which we are going to average. Equation (25) can be rewritten as  $(\nabla^2 - \kappa^2)\phi(\mathbf{r}) = 0$ , with  $\kappa \equiv c(q)/(r + \bar{r})$ . This is equivalent to an  $r$ -dependent screening radius, i.e.

$$R_{\text{scr}}(r) = \frac{r + \bar{r}}{c(q)}. \quad (33)$$

As shown in Figs. 3, the deviation of the potential (30) from the pure Coulomb form in the region of small relative pion momentum  $q \leq 30$  MeV, is small ( $b \rightarrow 0$ ). Since,  $\kappa \rightarrow 0$  when  $v_{\text{rel}} \ll 1$  (see Eq. (28)), we first ignore the  $r$  dependence of  $\kappa$  to obtain the solution for the electromagnetic  $\pi\pi$  potential in the form of Eq. (8), then substitute the  $r$ -dependent  $\kappa$  into Eq. (8), to find that

$$U_{\pi\pi} = \frac{\alpha e^{-c(q)r/(r+\bar{r})}}{r} \quad (34)$$

no longer decreases exponentially with distance when  $r$  is large enough  $r \gg \bar{r}$ . Instead, the numerator on the r.h.s. of Eq. (34) represents the averaged charge distribution (32) squared (we are now considering the potential energy  $U_{\pi\pi}$  rather than the electric potential  $\phi$ , hence the extra factor of charge leading the  $\alpha$ ).

It is clear from Eq. (28) that if  $v_{\text{rel}}/v_{\text{cm}} \ll 1$  ( $R_f$  and  $R_{\text{scr}}^f$  are of the same order for high multiplicities) the renormalized constant  $\alpha_{\text{eff}} = \alpha \exp[-c(q)]$  is close to the bare value of  $\alpha$ . Moreover, the same qualitative result comes from the  $r$ -behaviour of the screening radius (33) when it approaches the asymptotic value  $R_{\text{scr}} = \infty$  (Coulomb law) with increasing  $r$ . The quantity  $c(q)$  increases with relative pion momentum, leading to larger deviations from the Coulomb potential and agreement with the features of the potential (30) (see discussion after Eq. (31)).

### 3.1 Evaluations

The numerical evaluations of the correction factor (Gamov factor) should be provided by the solution of the Schrödinger equation with the potential

$$U_{\text{expan}}(r) = \frac{\alpha}{r} \left( \frac{\bar{r}}{r + \bar{r}} \right)^b, \quad (35)$$

where the exponent  $b$  is momentum-dependent, in accordance with (31). Then, one can construct the correction factor  $G_{\text{cor}}(|\mathbf{q}|) = |\psi_{\mathbf{q}}(\mathbf{r} = 0)|^2$ . To compare it with the standard



Gamov factor  $G_0$  we calculate the ratio  $G_0/G_{\text{cor}}$  for the LHC freeze-out conditions. The results are depicted in Fig. 4 as dotted curves for three different values of the pair mean momentum  $P_{\text{cm}}$ .

We now correct the two-particle potential (35) for small distances  $r \leq a \equiv n_f^{-1/3}$ , where  $n_f$  is the freeze-out pion density, i.e. in the region where the distance  $r$  between two pions is smaller than the mean distance between the particles in the gas. Indeed, there is no ‘screening’ effect for this distance, and hence the potential should be the Coulomb one. There is no such a problem for the statically screened potential  $U(r) = \alpha \exp(-r/R_{\text{scr}})/r$ , because the screening radius obeys the condition  $a \ll R_{\text{scr}}$  (by definition in the sphere  $4\pi R_{\text{scr}}^3/3$  the number of particles is much larger than 1); for the region  $r \leq a \ll R_{\text{scr}}$ , the potential  $U(r)$  automatically transforms into the Coulomb one,  $U(r) = \alpha/r$ . In the expansion scenario we have in addition to  $R_{\text{scr}}$  another scale parameter,  $\bar{r} = R_f (v_{\text{rel}}/v_{\text{cm}})$ , where  $R_f$  is the freeze-out size of the system ( $R_f = 7 - 10$  fm for *SPS* and *LHC* freeze-out conditions). By construction the potential  $U_{\text{expan}}(r)$  approaches the Coulomb one if (i)  $r \ll \bar{r}$  (see (35)). On the other hand, the scale parameter  $\bar{r}$  may be smaller than the mean distance between particles in the gas (ii)  $\bar{r} < a$ . In Fig. 5 we depict  $\bar{r}$  for different mean momenta of the pair:  $P_{\text{cm}} = 50, 150, 450$  MeV/c and for the mean distance between particles at freeze-out  $a = n_f^{-1/3}$  (horizontal lines). For instance, as is seen in Fig. 5, for  $P_{\text{cm}} = 450$  MeV/c and relative momentum  $q < 60$  MeV/c, we have  $\bar{r} < a$  for *SPS* freeze-out conditions. Hence, combining (i) and (ii) we get that the asymptotic regime, i.e. the Coulomb potential, can be achieved only for  $r \ll a$ . But we know that for separation distances which obey  $r < a$ , all distortions of the Coulomb potential vanish. Thus, the behaviour of the potential (35) must be corrected, since it should be a Coulomb one at distances that are smaller than the mean distance between particles. To improve the behaviour of the potential for distances smaller than  $a$ , we use a smooth ‘potential switcher’

$$s(x) = \frac{1}{2} - \frac{1}{2} \tanh[2(x-2)] , \quad (36)$$

which is depicted in Fig. 6. Then, incorporating the correct behaviour of the potential at small distances, we finally obtain the potential energy in the following form

$$U_{\pi\pi}(r) = s\left(\frac{r}{a}\right) \frac{\alpha}{r} + \left[1 - s\left(\frac{r}{a}\right)\right] U_{\text{expan}}(r) . \quad (37)$$

Certainly, with increasing time the mean distance between particles increases, and the Coulomb potential is thus switched on at distances larger than the freeze-out particle mean distance  $n_f^{-1/3}$ . But we restrict our calculation to the freeze-out mean distance. It means that in the competition between the two potentials  $U_{\text{Coulomb}}$  and  $U_{\text{expan}}$  we overestimate the contribution of the distorted potential  $U_{\text{expan}}$  and hence we overestimate the influence of the multiparticle environment.

The results of the calculation with potential (37) are shown for the *LHC* freeze-out conditions as solid curves in Fig. 4. The same ratio  $G_0/G_{\text{cor}}$  for the *SPS* freeze-out conditions is given in Fig. 7. The correction factor we obtained reveals only small deviations from the standard Gamov factor. This result can be explained by a fast decrease of the density of secondary particles with increasing distance of the pair from the fireball, which in turn results in a very small distortion of the two-particle Coulomb potential.

It is instructive to point out that evaluations that were made by the authors in [9] on the basis of a quasi-classical approximation are in good qualitative agreement with the present results.

## 4 Summary and conclusions

In our first approach (static scenario) it was assumed that the whole position space is filled by secondary pions with constant density. This uniform environment of secondary pions results in a screened two-pion Coulomb potential. We showed that for future LHC and RHIC experiments the screening radius of the Coulomb interaction at the freeze-out density is of a size comparable with the source, and therefore the factorization of Eq. (3) [2] is no longer valid. Moreover, solutions of the Schrödinger equation produce a correction factor  $G_{\text{cor}} = |\psi_{\mathbf{q}}(\mathbf{r} = 0)|^2$  which noticeably deviates from the standard Gamov factor (see Fig. 1). However, as we showed further, this model is a quite unrealistic approximation and is not relevant to the real picture of an expanding pion system after freeze-out.

The conclusions reached with the first model change drastically after passing to a more realistic model of an expanding pion system. In the second model, we first reduce the time evolution of the multipion post-freeze-out environment to a stationary one, parametrizing the density of the secondary pions  $n_{\pi}(t, R)$  for all times  $t$  as  $n(R) = \text{const}/R^2$ , where  $R$  is the distance from the fireball. The ‘constant’ is determined by the particular freeze-out conditions, namely it should be normalized on the real pion density  $n_f$  at the time of freeze-out. This parametrization results from the inequality  $n_{\pi}(t, R) \leq \text{const}/R^2$ , where equality is reached for an expanding system in which the radial particle velocities are all equal. Quite obviously, owing to the particle velocity dispersion, this parametrization is an overestimation of the real post-freeze-out pion density at any time  $t$ . Consequently, adopting this model of the pair environment, we overestimate the deviation from the Coulomb potential and thus overestimate the deviation from the Gamov factor. A further reduction results from the time evolution of the mean radii:  $R(t)$ , which is the distance of the separate pion pair c.m.s. from the fireball centre, and  $r(t)$ , which is a classical distance between these pions. Exploiting that reduction, we parametrize the relative motion, as well as the pair c.m.s. motion, by one variable  $r$ , thus eliminating the time dependence. After these reductions only one independent variable  $r$  is left.

It should be pointed out that the time derivatives can also be included into our consideration. From the  $r$ -parametrization, we obtain a proportionality of the time derivative to the pion–pion relative velocity  $v_{\text{rel}}$ , namely  $\frac{\partial}{\partial t} = v_{\text{rel}} \frac{\partial}{\partial r}$ . Since we are interested only in the small relative pion momenta this derivative can be neglected for a first-order estimate.

So, we reduce the problem to a stationary one where, in contrast to the first scenario, the pion pair moves after freeze-out in a non-uniform environment. Effectively, this means that we consider the problem in the two-pion rest frame, where the relative radial motion of the particles that create the environment is slow enough with respect to the radial expansion. Practically it allows us to consider the stationary Schrödinger equation instead of the time-dependent one. We show that the main contribution to the behaviour of the correction factor comes from the behaviour of the potential at the large distances that separate interacting particles. On the other hand, the interacting particles are separated by large distances when

they are far enough from the fireball (this statement is a basis of the  $r$ -parametrization). Hence, because of a very fast decrease of the density with respect to the distance from the fireball  $R$ , namely  $n(R) = \text{const}/R^2$ , the density of secondaries is small or even negligible at these distances. At this stage of the evolution, the long-range part of the potential is just the Coulomb one and it is responsible for the behaviour of the correction factor at small relative momentum  $q \leq 50$  MeV/c. That is why the correction factor for this region of relative pion momentum practically coincides with the Gamov one. The short-range behaviour of the potential (when  $r$  is smaller than a mean distance between the particles that form the environment), which is the Coulomb one for point-like pions, provides also only small deviations of the correction factor  $G_{\text{cor}}$  from the standard Gamov factor  $G_0$  for a large pion relative momentum  $q \geq 50\text{--}70$  MeV/c, as can be seen in Figs. 4 and 7.

For the high “*LHC*” freeze-out pion density  $n_f = 0.25 \text{ fm}^{-1/3}$  the reduction of the correction factor  $G_{\text{cor}}$ , as seen in Fig. 4, to the standard Gamov factor  $G_0$  increases with decreasing  $v_{\text{rel}}/v_{\text{cm}}$ , the ratio of the relative velocity of the detected pions to their c.m. velocity in the fireball rest frame. When this parameter is much less than unity, the pion pair promptly escapes the initial high-density region so that slow relative motion of the two pions takes place in an approximately empty spatial region and the distortion of the mutual Coulomb potential is weak.

This is not the case for “*SPS*” freeze-out conditions, as seen in Fig. 7. For the comparatively low pion density  $n_f = 0.03 \text{ fm}^{-1/3}$  the effect of small relative velocity is not pronounced because from the very beginning of the freeze-out the pions are not in such a dense environment and even small c.m. velocities are quite sufficient to bring the pair promptly into regions where the influence of the environment is negligible.

**Acknowledgements** D.A. acknowledges helpful discussions with G. Baym, D. Ferenc, V. Zasenkov and would like to express special thanks to U. Heinz, C. Slotta and J. Sollfrank who read the manuscript and made a number of remarks to improve the presentation.

## References

- [1] D.H. Boal, C.-K. Gelbke and B.K. Jennings, Rev. Mod. Phys. **62**, 553 (1990).
- [2] M. Gyulassy, S.K. Kauffmann and L.W. Wilson, Phys. Rev. C **20**, 2267 (1979).
- [3] D. Anchishkin, U. Heinz and P. Renk, Phys. Rev. C **57**, 1428 (1998) (Los Alamos e-print archive: nucl-th/9710051).
- [4] D. Anchishkin and G. Zinovjev, Phys. Rev. C **51**, R2306 (1995).
- [5] H.W. Barz, Phys. Rev. C **53**, 2536 (1996).
- [6] H.W. Barz, J.P. Bondorf, J.J. Gaardhøje and H. Heiselberg, Los Alamos e-print archive: nucl-th/9711064.
- [7] A.D. Sakharov, Soviet Phys.-JETP **18**, 631 (1948).

- [8] V.N. Baier and V.S. Fadin, Soviet Phys.-JETP **57**, 225 (1969).  
 [9] D.V. Anchishkin, W.A. Zajc and G.M. Zinovjev, Ukrainian J. Phys. **41**, 363 (1996)  
 (Los Alamos e-print archive: hep-ph/9512279).

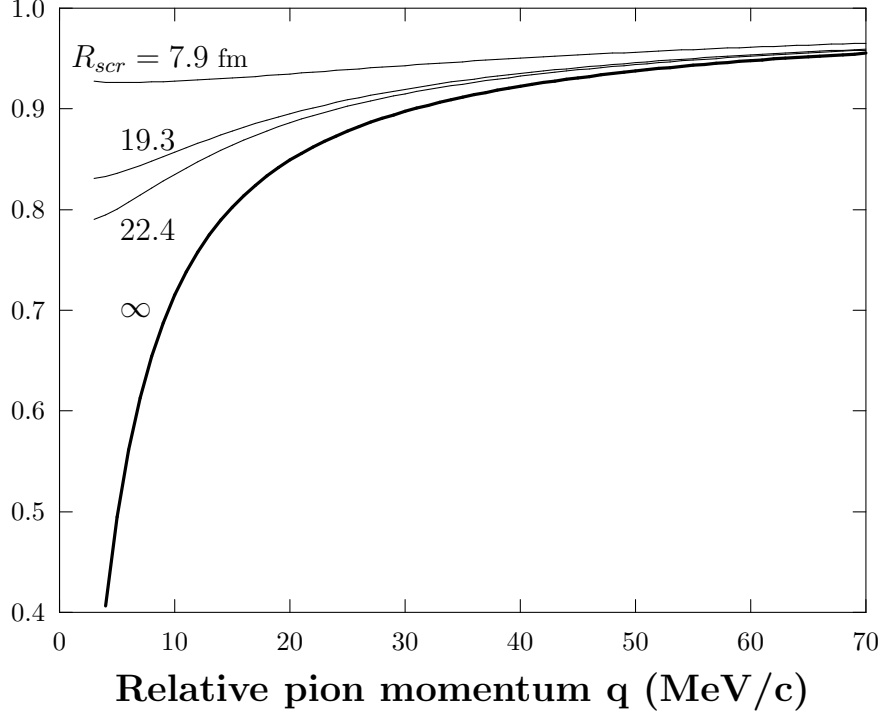


Figure 1: Correction factor  $G_{\text{cor}}(q) = |\psi_{\mathbf{q}}(\mathbf{r} = 0)|^2$  as a function of the relative pion momentum  $q = |\mathbf{q}|$  (MeV/c). Wave function  $\psi_{\mathbf{q}}(\mathbf{r})$  is the solution of the Schrödinger equation for the screened Coulomb potential (10). Three curves correspond to different freeze-out conditions: 1) *LHC* freeze-out conditions:  $n_f = 0.25 \text{ fm}^{-1/3}$ ,  $T_f = 190 \text{ MeV}$ , and  $R_{\text{scr}} = 7.9 \text{ fm}$  (see Eq. (9)); 2) Intermediate case:  $R_{\text{scr}} = 19.3 \text{ fm}$ ; 3) *SPS* freeze-out conditions:  $n_f = 0.03 \text{ fm}^{-1/3}$ ,  $T_f = 190 \text{ MeV}$ , and  $R_{\text{scr}} = 22.4 \text{ fm}$ . Bottom curve is the standard Gamov factor,  $R_{\text{scr}} = \infty$ .

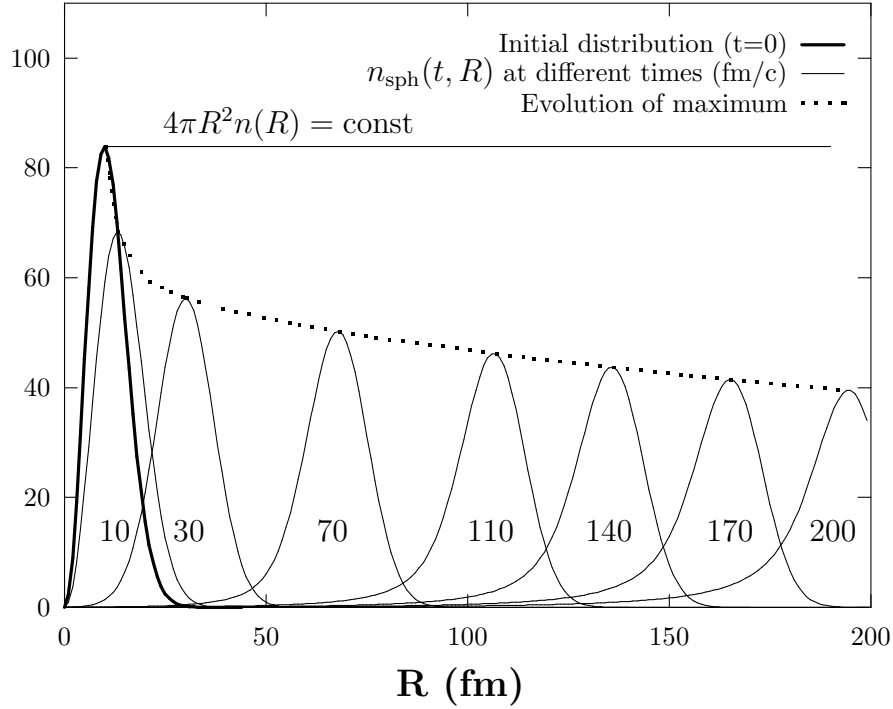


Figure 2: Dependence of the spherical pion density  $n_{\text{sph}}(t, R) \equiv 4\pi R^2 n(t, R)$  ( $\text{fm}^{-1}$ ) on  $R$ , where  $n(t, R)$  is the number of pions in the unit volume at time  $t$  and at distance  $R$  from the center of the fireball ( $\int_0^\infty dR n_{\text{sph}}(t, R) = N_\pi$ ). The density was evaluated for initial data associated with *SPS* freeze-out conditions:  $n_f = 0.03 \text{ fm}^{-1/3}$ ,  $R_f = 7.1 \text{ fm}$ ,  $T_f = 190 \text{ MeV}$ . The spherical pion density (solid Gaussian-like curves) is depicted for the times: 1)  $t = 0$ , initial distribution, 2)  $t = 10 \text{ fm/c}$ , 3)  $t = 30 \text{ fm/c}$ , 4)  $t = 70 \text{ fm/c}$ , 5)  $t = 110 \text{ fm/c}$ , 6)  $t = 140 \text{ fm/c}$ , 7)  $t = 170 \text{ fm/c}$ , 8)  $t = 200 \text{ fm/c}$ . The dotted curve is the evolution of the maximum of spatial pion distribution. The horizontal solid line at the top is a constant spherical density  $n_{\text{sph}}(t, R) = 4\pi R^2 n(R) = \text{const}$  ( $\text{fm}^{-1}$ ).

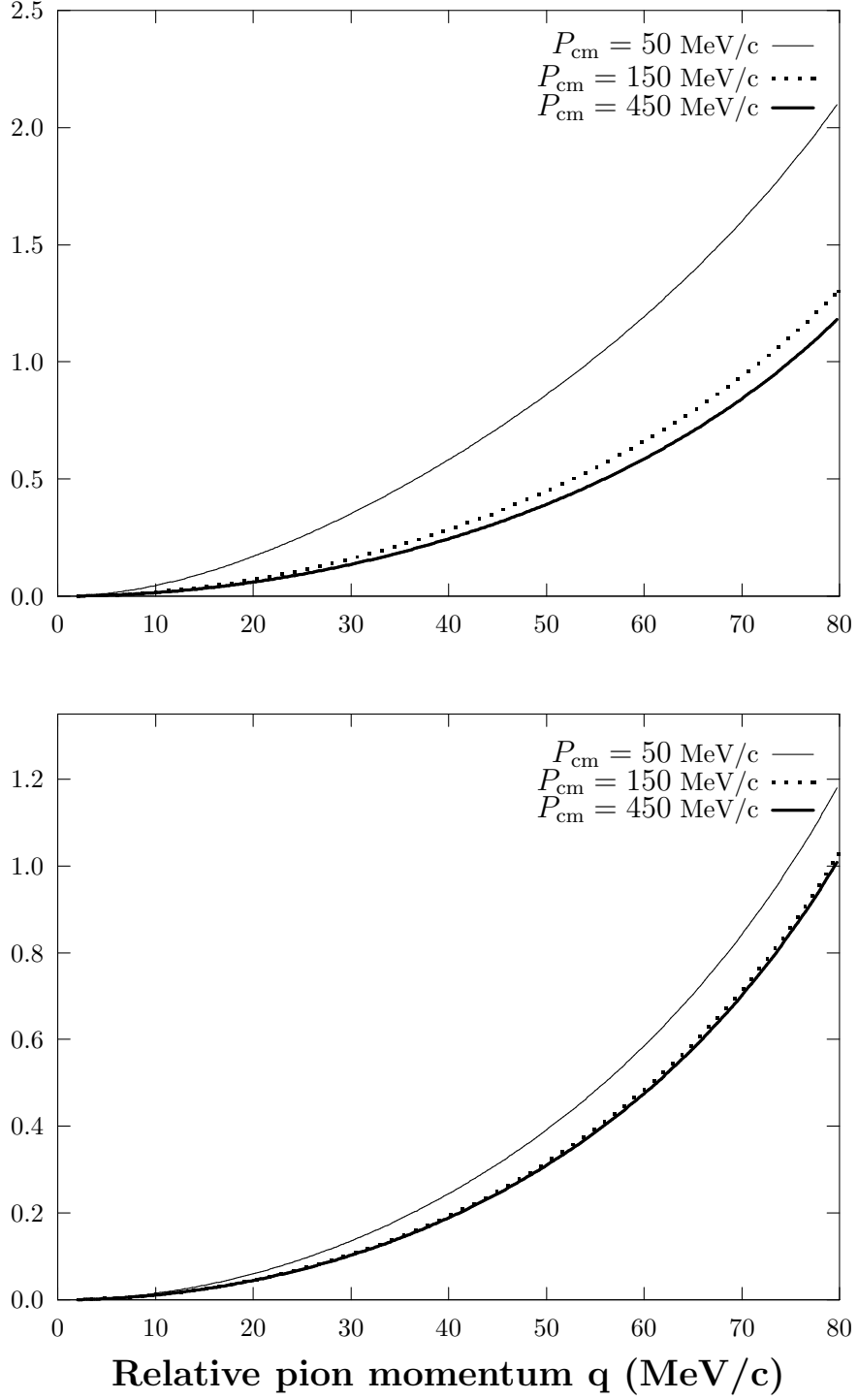


Figure 3: Exponent  $b(q)$  (see Eqs. (31) and (32))  
a) for the *LHC* freeze-out conditions:  $n_f = 0.25 \text{ fm}^{-1/3}$ ,  $T_f = 190 \text{ MeV}$ ;  
b) for *SPS* freeze-out conditions:  $n_f = 0.03 \text{ fm}^{-1/3}$ ,  $T_f = 190 \text{ MeV}$ .

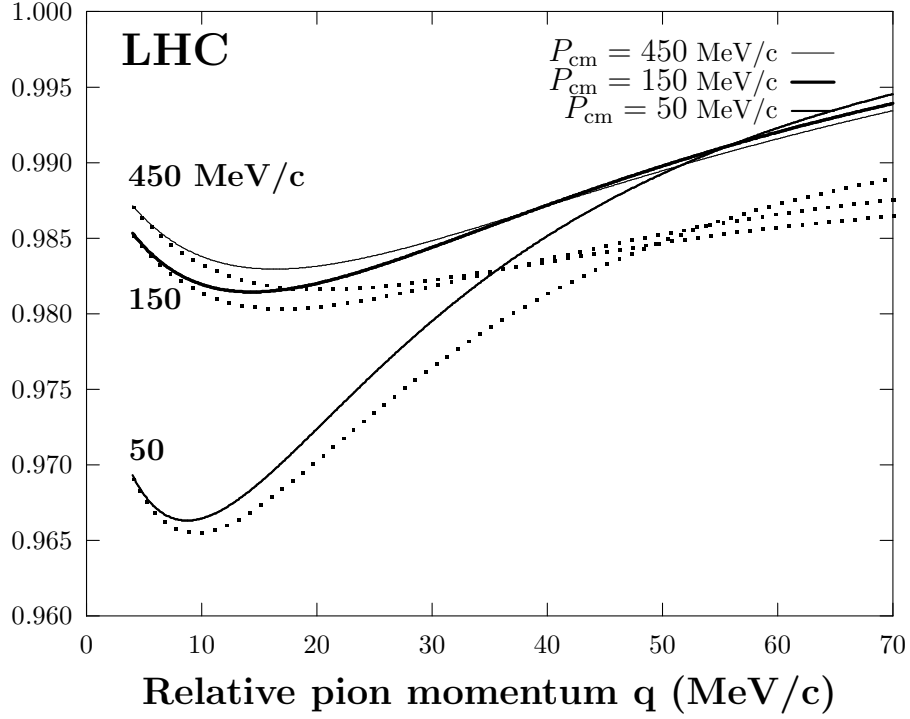


Figure 4: The ratio of the standard Gamov factor  $G_0$  to the correction factor  $G_{\text{cor}}(q) = |\psi_{\mathbf{q}}(\mathbf{r} = 0)|^2$  obtained from the solution of the Schrödinger equation for the *LHC* freeze-out conditions:  $n_f = 0.25 \text{ fm}^{-1/3}$ ,  $R_f = 7.1 \text{ fm}$ ,  $T_f = 190 \text{ MeV}$ .

The dotted curves show the evaluation made using the potential (36), the solid curves using the improved potential (38). The curves are drawn for different mean momenta of the pion pair  $P_{\text{cm}} = |\mathbf{p}_a + \mathbf{p}_b|/2$  in the fireball frame.

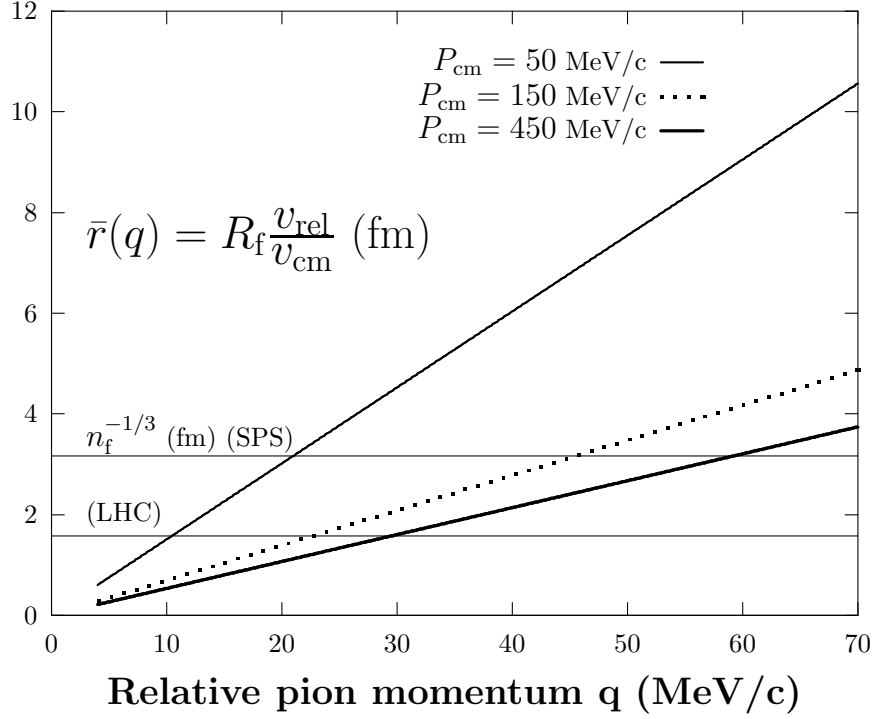


Figure 5: Dependence of the dynamical freeze-out radius  $\bar{r}(q) = R_f \frac{v_{rel}}{v_{cm}}$  (fm) on the relative pion momentum  $q$  (MeV/c). Slope lines are drawn for different mean momenta of the pair:  $P_{cm} = 50, 150, 450$  MeV/c. The mean distance between particles at freezeout  $a = n_f^{-1/3}$  (fm) are drawn as horizontal lines for *SPS* ( $a = 3.16$  fm) and *LHC* ( $a = 1.58$  fm) freeze-out conditions.



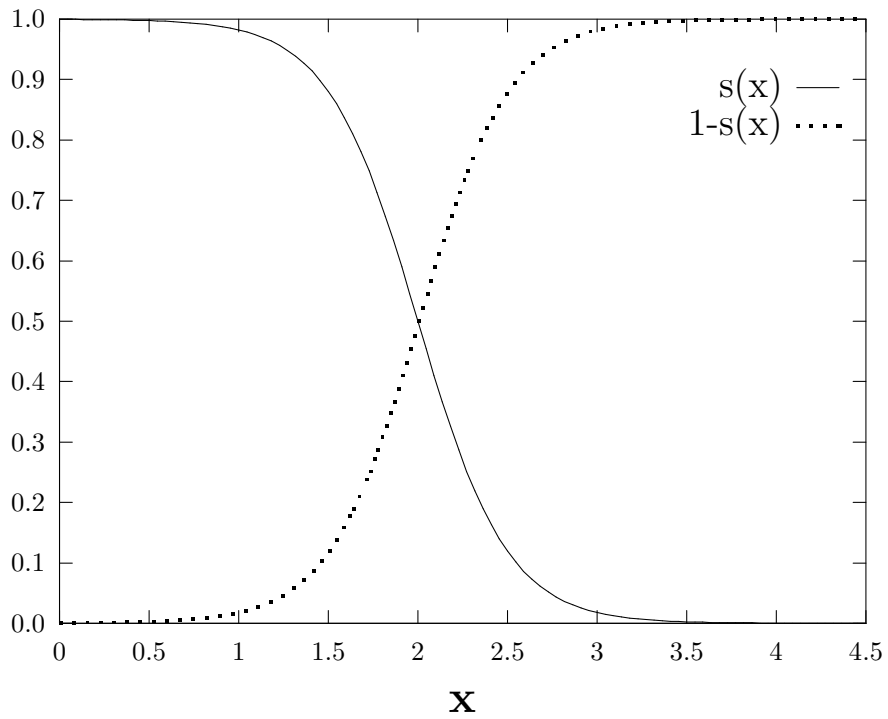


Figure 6: The solid curve is a smooth potential switcher  $s(x) = \frac{1}{2} - \frac{1}{2}\tanh[2(x-2)]$ . The dotted curve is an alternative potential switcher  $1-s(x)$ .

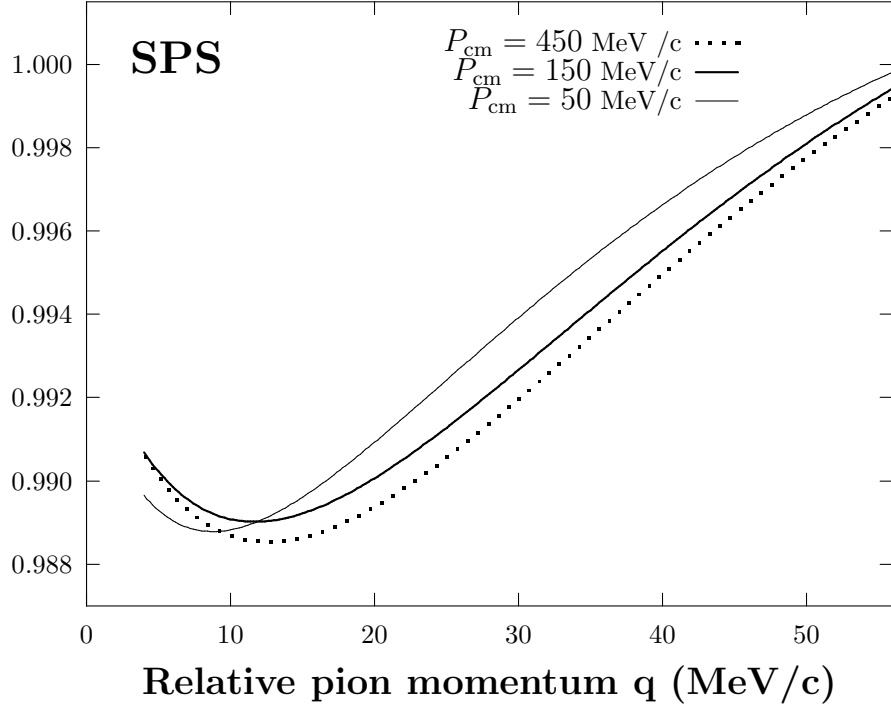


Figure 7: The ratio of the standard Gamov factor  $G_0$  to the correction factor  $G_{\text{cor}}(q) = |\psi_{\mathbf{q}}(\mathbf{r} = 0)|^2$  obtained from the solution of the Schrödinger equation, using the improved potential (38) for *SPS* freeze-out conditions:  $n_f = 0.03 \text{ fm}^{-1/3}$ ,  $R_f = 7.1 \text{ fm}$ ,  $T_f = 190 \text{ MeV}$ . The curves are drawn for different mean momenta of the pion pair  $P_{\text{cm}} = |\mathbf{p}_a + \mathbf{p}_b|/2$  in the fireball frame.